Numerical Techniques and Cloud-Scale Processes for High-Resolution Models

James D. Doyle
Naval Research Laboratory
Monterey CA 93943-5502
phone: (831) 656-4716 fax: (831) 656-4769 e-mail: doyle@nrlmry.navy.mil

Award Number: N0001407WX20951
http://www.nrlmry.navy.mil/projects/coamps

LONG-TERM GOALS

The long-term goal of this project is to design and evaluate the components that will comprise a next generation mesoscale atmospheric model within the Coupled Ocean/Atmosphere Mesoscale Prediction System (COAMPS®[1]). It is anticipated that in order to meet future Navy requirements, next generation approaches to numerical techniques and physical parameterizations will be needed.

OBJECTIVES

The objectives of this project involve the development, testing, and validation of: i) new numerical techniques such as advection schemes and time differencing methods, and ii) new methods for representing cloud-scale physical processes. Both of these objectives are tailored to address high-resolution applications for horizontal grid increments at 1 km or less.

APPROACH

Our approach is to follow a methodical plan in the development and testing of a nonhydrostatic microscale modeling system that will leverage the existing COAMPS and new model prototypes. Our work on numerical methods will involve investigation of spatial and temporal discretization algorithms that are superior to the current generation leap-frog, second-order accurate numerical techniques presently employed in COAMPS and many other models; these new discretization methods will be developed and implemented. Our work on the physics for the next-generation COAMPS will feature the development of physical parameterizations specifically designed to represent cloud-scale processes operating on fine scales. A parameterization is proposed that properly represents the coupled nature between the turbulence and microphysics in droplet activation, evaporation, and auto-conversion processes for mesoscale and microscale models. Validation and evaluation of the modeling system will be performed using datasets of opportunity, particularly in regions of Navy significance.

WORK COMPLETED

1. Development of a new parameterization of turbulent cloud droplet number density flux.
Prediction of cloud microphysics is a crucial part of next generation COAMPS; it depends on the realistic parameterization of turbulent mixing of cloud droplets. Traditionally, the turbulent mixing of the droplet number concentration is calculated based on the so-called down-gradient method in which the

[1] COAMPS® is a registered trademark of the Naval Research Laboratory.

Report Documentation Page

Form Approved
OMB No. 0704-0188

1. REPORT DATE	2. REPORT TYPE	3. DATES COVERED
30 SEP 2007	**Annual**	**00-00-2007 to 00-00-2007**

4. TITLE AND SUBTITLE	5a. CONTRACT NUMBER
Numerical Techniques And Cloud-Scale Processes For High-Resolution Models	5b. GRANT NUMBER
	5c. PROGRAM ELEMENT NUMBER
6. AUTHOR(S)	5d. PROJECT NUMBER
	5e. TASK NUMBER
	5f. WORK UNIT NUMBER
7. PERFORMING ORGANIZATION NAME(S) AND ADDRESS(ES) **Naval Research Laboratory,Monterey,CA,93943-5502**	8. PERFORMING ORGANIZATION REPORT NUMBER
9. SPONSORING/MONITORING AGENCY NAME(S) AND ADDRESS(ES)	10. SPONSOR/MONITOR'S ACRONYM(S)
	11. SPONSOR/MONITOR'S REPORT NUMBER(S)

12. DISTRIBUTION/AVAILABILITY STATEMENT
Approved for public release; distribution unlimited

13. SUPPLEMENTARY NOTES
code 1 only

14. ABSTRACT
The long-term goal of this project is to design and evaluate the components that will comprise a next genera-tion mesoscale atmospheric model within the Coupled Ocean/Atmosphere Mesoscale Prediction System (COAMPS?1). It is anticipated that in order to meet future Navy requirements, next generation approaches to numerical techniques and physical parameterizations will be needed.

15. SUBJECT TERMS

16. SECURITY CLASSIFICATION OF:			17. LIMITATION OF ABSTRACT	18. NUMBER OF PAGES	19a. NAME OF RESPONSIBLE PERSON
a. REPORT	b. ABSTRACT	c. THIS PAGE			
unclassified	**unclassified**	**unclassified**	**Same as Report (SAR)**	**11**	

droplets are diffused along the direction of decreasing concentration. This approach, however, is severely flawed, because it does not include key physical processes that are critical to the droplet spectrum evolution, i.e. the droplet activation in turbulent updrafts and the evaporation in the downdrafts. A new mixing scheme is developed to include these processes; it can be written as

$$\frac{\partial \overline{w'N'}}{\partial t} = Transport + dissipation + \left(\frac{\partial \overline{w'N'}}{\partial t} \right)_{act},$$

where $\overline{w'N'}$ is turbulent flux of the droplet number density, first two terms on the right-hand-side represents normal processes related turbulence transport and dissipation, and the last is the activation contribution to the flux. The activation term is formulated in terms of the probability density function of vertical velocity and aerosol activation spectrum. This term makes significant contribution at the cloud base where the activation occurs in the updrafts. Therefore, the turbulent flux is closely coupled to the turbulence structure. We included this parameterization in a single column high-resolution turbulence closure model and tested the performance against DYCOMS (Dynamics and Chemistry of Marine Stratocumulus Cloud Experiment II) observations.

2. New lower boundary condition for the COAMPS dynamical core

Over the past several years, a negative geopotential height bias has been apparent in the COAMPS model during wintertime months. This height bias was particularly apparent in mid-latitude regions such as the FNMOC operational Europe area. Height biases of -50 m at 500 hPa were common the wintertime months and much larger than the NOGAPS height biases. Over the past year, a series of real data and simplified tests were run using COAMPS, the results of which motivated the implementation of a new lower boundary condition for the COAMPS nonhydrostatic model.

3. Spectral element and discontinuous Galerkin 2D prototypes.

In FY07 we continue examination of three different nonhydrostatic equation sets and explore solving these equation sets using spectral element and discontinuous Galerkin techniques. We have continued collaboration with Frank Giraldo at NPS with this work. Spectral element (SE) (see Giraldo 2005) and discontinuous Galerkin (DG) (see Giraldo 2006) methods are a new class of spatial discretization methods that are used to approximate the derivatives of the governing equations. The advantage of SE and DG methods is that they offer high-order accuracy and this accuracy can be achieved on any unstructured grid – this is not true for finite difference methods where the differencing stencils require a certain level of structure (such as orthogonality). Based on SE and DG methods, we examined 5 different prototypes for the nonhydrostatic Euler equations. We tested various aspects of these models using idealized cases for warm bubbles, gravity currents, and gravity waves.

4. Development of new cloud microphysical equations with variable collection efficiencies

For many applications of interest, it is necessary to consider mixed-phase cloud microphysical processes. In standard bulk cloud microphysical schemes, collection rates are computed between the ice and liquid condensate categories with the result often being the creation a third condensate category (such as rain and snow collisions leading to the formation of graupel). Such rate calculations have been shown to lead to the over-depletion of the collected scalar within a given time step (referred to as the over-depletion problem). Modelers typically resort to placing add hoc limits to the rate equations to preserve a positive-definite solution. A recent study by Gaudet and Schmidt (2007) analyzed the nature of these errors and derived a new formulization of the rate equations, termed “Numerical Bound-

ing", which is based on accurate numerical integration of the collection terms. The new equations accurately account for errors in the standard time discretization of the collection equations allowing much larger time steps to be taken, a fact which may prove useful for envisioned semi-Lagrangian numerical frameworks. We have now extended these results to include variable collection efficiencies that account for known drop/crystal interactions. The work has involved developing a parameterization of the collection efficiency calculations of Wang and Ji (2000) for a variety of crystal and droplet diameters.

5. Weighted Essentially Non-Oscillatory (WENO) methods.
Atmospheric models require numerical methods that can accurately represent the transport of tracers with steep gradients, such as those that occur at cloud boundaries or the edges of chemical plumes. In atmospheric sciences, the most widely used numerical techniques for this type of problem are flux-corrected transport or closely related flux-limiter methods. The limiters are typically designed to prevent the development of new extrema in the concentration field. This will preserve the non-negativity of initially non-negative fields, which is essential for the correct simulation of cloud microphysics or chemical reactions. One serious systematic weakness of flux limiter methods is that they also tend to damp the amplitude of extrema in smooth regions of the flow, such as the trough of a well-resolved sine wave. To avoid this problem, we have been investigating the application of WENO (Weighted Essentially Non-Oscillatory) methods to tracer transport in atmospheric models. WENO methods are widely used in many disciplines, but scarcely been tested in atmospheric applications. WENO methods preserve steep gradients while simultaneously avoiding the dissipation of smooth extrema by estimating the value of the solution in a way that heavily weights the smoothest possible cubic polynomial fit to the local function values. Where the solution is well resolved, all possible cubic interpolants are weighted almost equally. Near a steep gradient, those interpolants are almost completely ignored.

RESULTS

1. Development of a new parameterization of turbulent cloud droplet number density flux.
Fig. 1 shows the comparison of the results between the old and new parameterizations. The traditional "down-gradient" scheme predicts lower cloud droplet number density than the new parameterization; the result predicted by the new scheme is closer to the observation (circles with horizontal bars). This difference comes from the different treatment in the turbulent droplet number flux. The old "down-gradient" approach diffuses significant amount of droplets down to the cloud base where they are evaporated and exit clouds; the new scheme produces "up-gradient" flux profile because of the activation in the updrafts, leading to upward transport of the droplets within cloud layer. It is seen that the new flux scheme indeed improves the cloud microphysical prediction. The parameterized turbulent flux is also compared with that computed from NRL COAMPS-LES model. Since a LES model can explicitly resolve the stochastic motion of turbulent eddies, it can correctly simulate the droplet number flux. Thus COAMPS-LES provides a basic evaluation of the parameterization result. It is seen in Fig. 2 that the parameterized turbulent flux profile is very close to that from COAMPS-LES. Both COAMPS-LES and the new parameterization predict the "up-gradient" feature just above the cloud base, which further confirms our view that the new method is more realistic than the old down-gradient approach.

2. New lower boundary condition for the COAMPS dynamical core
During FY07, a series of real data and simplified tests were run using COAMPS in order to determine the source of a geopotential height bias. After a series of intensive sensitivity tests, it was determined

that the formulation of the lower boundary condition for the vertical velocity equation was the cause of the geopotential height bias. Three different formulations were tested for the lower boundary condition. A second order finite difference technique was found to produce the best results with the lowest height bias statistics. For example, the mean sea level pressure bias, shown in Fig. 3, for the period 1-14 February 2007 indicates that the new lower boundary condition reduces the sea level pressure bias by approximately 50% for the Europe operational area. The geopotential height bias and RMS errors in the troposphere were reduced considerably by 50% or more.

3. Spectral element 2D prototypes.

In order to determine which equation set along with which numerical method is best suited for building a next-generation mesoscale model, we ran simulations for a number of standard test cases. Here we illustrate one of these test cases for linear hydrostatic waves using the spectral element dynamical core with equation set. The setup of the computational grid was modified to allow for an arbitrary stretching of grid elements in both vertical and horizontal direction. Consecutively, the spatial resolution (either vertical or horizontal) is refined in elements with smaller extent. In the example shown (Fig. 4), the stretching was applied in both horizontal and vertical direction and the grid elements are shallower closer to the bottom boundary, and narrower closer to the obstacle at the center of the domain. The finer spatial resolution in areas of interest (e.g. boundary layer, lee slope of the mountain) also puts an additional restriction on the time step of the model, on top of the temporal restriction due to irregularly spaced nodal points within each element. In this example, the polynomial order was 8 in both directions. The simulation depicts a linear hydrostatic mountain wave case in an isentropic atmosphere, with a small obstacle (height = 1 m, half-width = 10000 m) at the center of the domain. The vertical velocity, shown in Fig. 5, agrees with analytic solutions, even with the coordinate stretching.

4. Development of new cloud microphysical equations with variable collection efficiencies

Figure 6 shows the collision efficiency as computed by Wang and Ji (2000) together with the parameterized efficiency for a crystal radius of 800 microns. The plots show the rapid increase of the drop/ice collision efficiency (ESR) to a value near 1.0 as the droplet size increases beyond about 30 microns. The ESR values remain steady near the maximum until the drop fall speed approaches that of the given crystal at which point the ESR values rapidly fall to zero. An inspection of Fig. 6a reveals that ESR remains fixed at a value of zero for all droplets greater than the critical diameter. A study of drop-drop interactions by Pinsky et. al. 2001 suggests that the collision efficiencies may rapidly increase again beyond this critical threshold to a value near one as the larger faster moving drops collide with the smaller drops. We thus seek to test the impact of a similar effect in our drop/crystal collision efficiency parameterization caused by faster moving droplets impacting slower moving crystals. The effects of applying a variable ESR to the case of rain collecting snow are shown in Fig. 7. The Figure shows that by far the greatest over-depletion arises from the standard analytical solution (ESR = 1.0) as it appears in our operational COAMPS code (solid line labeled A). By invoking a numerical solution of the rain/snow collection while retaining a fixed ESR = 1.0, we find that the over-depletion is effectively eliminated for a wide range of rain mixing values (curve B). This reduction results in large part from the removal of the so-called Wisner approximation during the numerical integration (in the analytical solution, the velocity differences between each species are assumed constant and removed from the integration). Including the numerical bounding technique (yet keeping a fixed ESR = 1.0) completely eliminates the over-depletion as demonstrated by Gaudet and Schmidt (2007) [curve C]. Finally, adding a variable ESR as depicted in Fig. 7 to the numerically bounded solution results in a further reduction of this particular rate calculation to a value quite near zero (curve D). Comparing D with A we find well over an order of magnitude reduction in this calculation (a known graupel source

term). By allowing ESR to return to a value of one beyond the critical drop radius, however, leads to nearly an identical solution to that of curve C. This suggests that a variable ESR will have its greatest impact on snow or pristine ice collisions with cloud droplet due to the slower droplet fallspeeds.

5. Weighted Essentially Non-Oscillatory (WENO) methods

We have developing a new method, in which WENO like criteria for the presence of poorly resolved steep gradients are evaluated in a highly efficient manner and used to determine whether spurious new maxima and minima are likely to be created in the vicinity of a steep gradient. This new approach, which we call "selective limiting," can be applied to both flux-corrected transport (FCT) methodologies or to piecewise polynomial approximations for the fluxes in finite-volume methods, particularly the piecewise parabolic (PPM) or cubic methods (PCM). Over a wide range of tests, these schemes were found to give more accurate solutions than WENO methods for considerably less computational cost.

Figure 8 shows the basic behavior of the exact solution. An initially round concentration of chemical tracer is deformed into a crescent in a sheared circular flow. At t=0, the flow in the outer part of the domain is faster, and the flow near the center is slower, than that associated with solid body rotation. However the strength of the sheared component of the flow periodically reverses to that at every multiple of T/2 time units, the total circular arc traveled by each fluid parcel is identical to that for one revolution of solid body rotation, and the correct tracer field distribution is exactly the same as the initial condition. Figure 9 compares numerical results generated by: (a) the unlimited PCM method, (b) the selectively limited PCM method with positivity preservation, (d) the standard WENO method, and (e) the selectively limited PCM method using a semi-Lagrangian framework with a maximum CFL number of 4. The total error in the mean-square sense (E_2) and the maximum norm (E_∞) is plotted in the lower left of each panel, the maximum and minimum values of the numerical solution (which can be compared with the correct values of 0 and 1) are plotted in the lower right. Both the Eulerian and semi-Lagrangian methods are performing better than the WENO method. At least as significant are the timing comparisons for this test, which show that the WENO method is a factor of 5 slower than the Eulerian selectively limited PCM method and a factor of 20 slower than the semi-Lagrangian PCM. This method is slightly faster and considerably more accurate than the semi-Lagrangian FCT method being incorporated into the WRF model(Skamarock, 2006). The four leftmost panels in Fig. 9 all show results from simulations at relatively coarse resolution (50x50 gridpoints). At finer resolutions of 100x100 (Fig. 9c) or 200x200 (Fig. 9f), the selectively limited PCM method yields considerably more accurate results and converges in proportion to the fifth order of the grid spacing.

IMPACT/APPLICATIONS

COAMPS is the Navy's operational mesoscale NWP system and is recognized as the key model component driving a variety of DoD tactical decision aids. Accurate mesoscale prediction is considered an indispensable capability for defense and civilian applications. Skillful COAMPS predictions at resolutions less than 1 km will establish new capabilities for the support of the warfighter and Sea Power 21. Operational difficulties with weapon systems such as the Joint Standoff Weapon (JSOW) have been documented in regions with fine-scale topography due to low-level wind shear and turbulence. Improved high-resolution predictive capabilities will help to mitigate these problems and introduce potentially significant cost saving measures for the operational application of JSOW. The capability to predict the atmosphere at very high resolution will further the Navy sea strike and sea shield operations, provide improved representation of aerosol transport, and will lead to tactical model improvements.

This research will establish important direction for the development of the Navy's next generation microscale prediction system. Emergency response capabilities and Homeland Security issues within the DoD and elsewhere, such as LLNL, will be enhanced with the new modeling capability.

TRANSITIONS

The next generation COAMPS system will transition to 6.4 projects within PE 0603207N (SPAWAR, PMW-180) that focus on the transition COAMPS to FNMOC. The improvements to the COAMPS dynamical core have been transitioned to the SPAWAR 6.4 project and subsequently to operations as a result of the marked improvement in the geopotential height bias statistics.

RELATED PROJECTS

COAMPS will be used in related 6.1 projects within PE 0601153N that include studies of air-ocean coupling, boundary layer studies, and topographic flows, and in related 6.2 projects within PE 0602435N that focus on the development of the atmospheric components (QC, analysis, initialization, and forecast model) of COAMPS.

REFERENCES

Gaudet, B.J. and J.M. Schmidt, 2007: Assessment of hydrometeor collection rates from exact and approximate equations. Part II: Numerical Bounding. *J. Appl. Met. Clim*., **46**, 82-95.

Giraldo, F. X., 2005: Semi-implicit time-integrators for a scalable spectral element atmospheric model. *Q. J. R. Meteorol. Soc*., **131**, 2431-2454.

Giraldo, F. X., 2006: High-order triangle-based discontinuous Galerkin methods for hyperbolic equations on a rotating sphere. *Journal of Computational Physics*, **214**, 447-465.

Hodur, R. M., 1997: The Naval Research Laboratory's Coupled Ocean/Atmosphere Mesoscale Prediction System (COAMPS). *Mon. Wea. Rev.*, **125**, 1414-1430.

Pinsky, M. A. Khain, and M. Shapiro, 2001: Collision efficiency of drops in a wide range of Reynolds numbers: Effects of pressure on spectrum evolution. *J. Atmos. Sci.*, **58**, 742-764.

Skamarock, W, 2006: Positive-definite and monotonic limiters for unrestricted-time-step transport schemes. *Mon. Wea. Rev*., **134**, 2241-2250.

Wang, P.K. and W. Ji, 2000: Collision efficiencies of ice crystals at low-intermediate Reynolds numbers colliding with supercooled cloud droplets: A numerical study. *J. Atmos. Sci*. **57**, 1001-1009.

PUBLICATIONS

Blossey, P.N. and D.R. Durran, 2007: A simple, effective WENO-like smoothness metric for use in conservative models of scalar advection. J. Comput. Phys., accepted subject to revision.

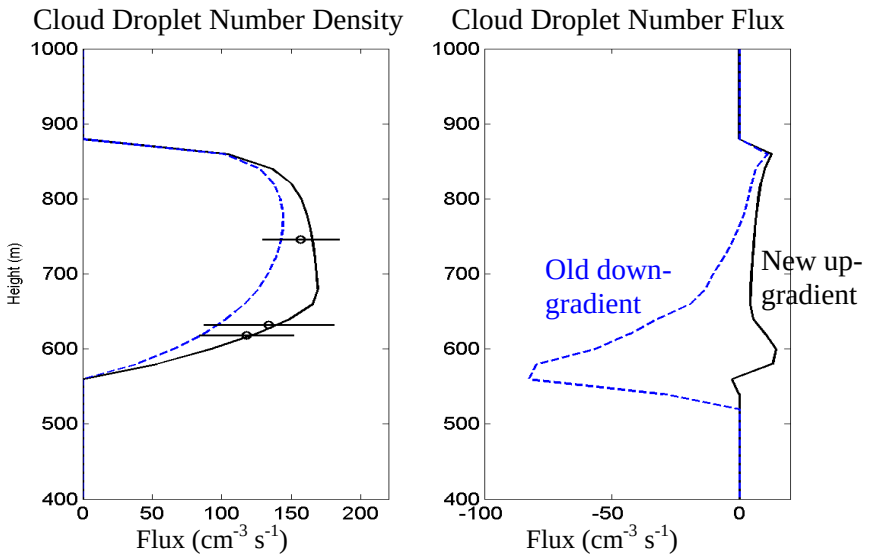

Figure 1. The model simulation of the cloud droplet density (left panel) and the turbulent flux (right panel) of the droplet density in a DYCOMS II observation case. Blue lines represent the result from the traditional "down-gradient" parameterization; black lines that from the new parameterization. The circles are the leg averages of the aircraft data taken in DYCOMS II flight 1; and horizontal bar is the scatter of the data.

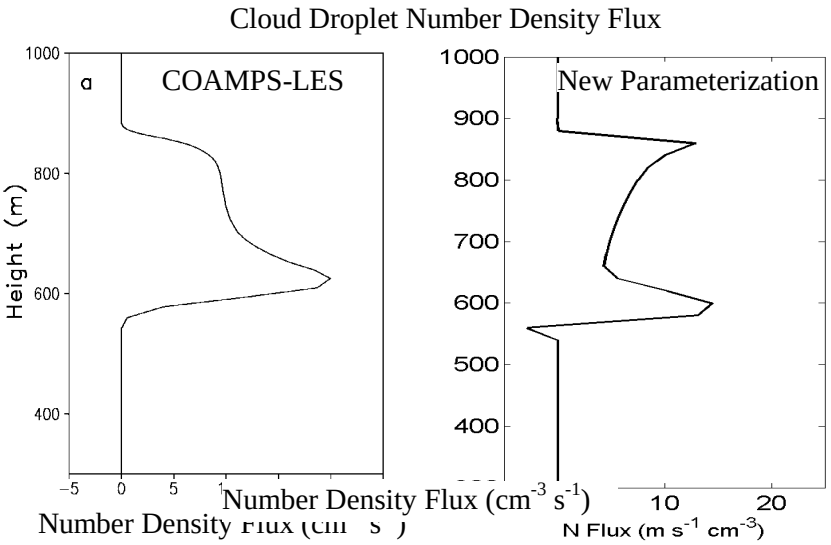

Figure 2. Comparison of the flux between COAMPS-LES results (left panel) and the new parameterization (right panel).

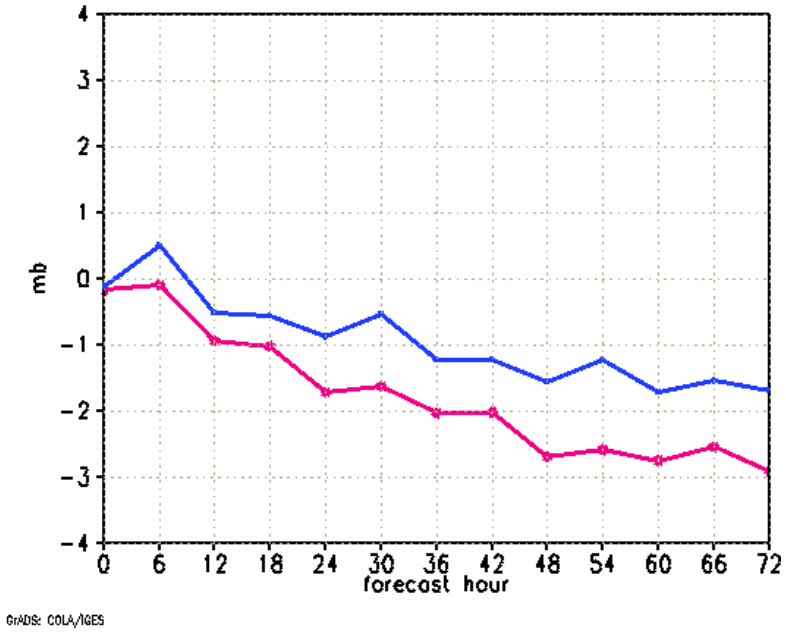

Figure 3. Mean sea level pressure bias as a function of forecast hour for Feb. 1-14, 2007 for the control (red) and new lower boundary condition for vertical velocity (blue) forecasts. Only the forecasts initialized at 00 UTC were included in this figure.

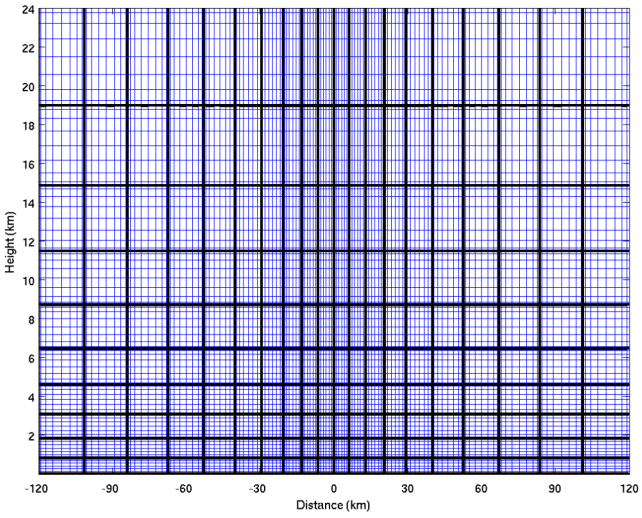

Figure 4. Grid elements (thick black lines) and computational grid (thin blue lines).

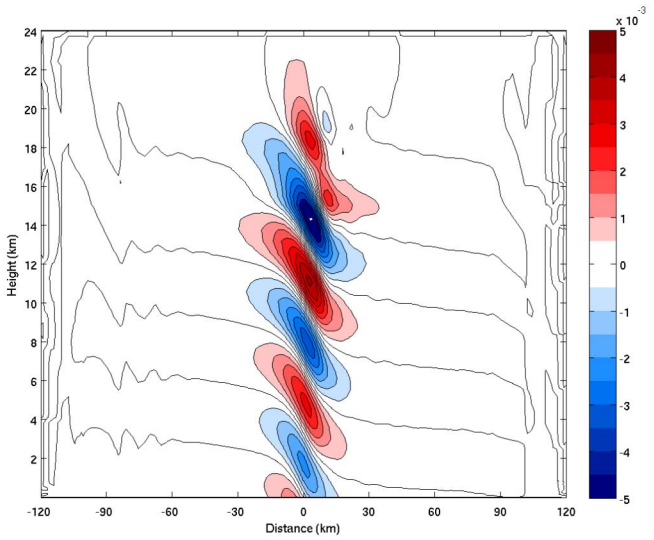

Figure 5. Perturbation vertical velocity (m s^{-1}) after 24 h of integration.

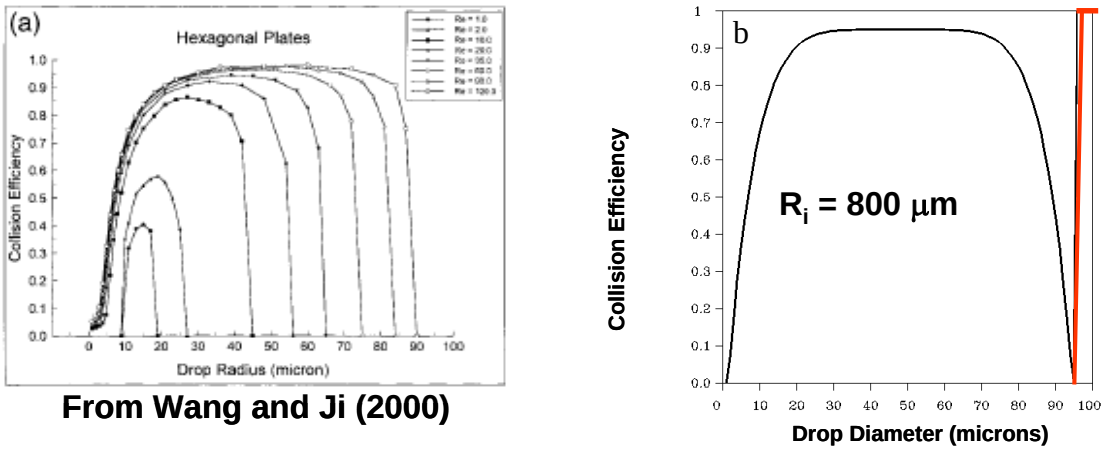

Figure 6. Collisional efficiencies of hexagonal ice plates colliding with supercooled droplets as (a) computed numerically by Wang and Ji (2000) and (b) as parameterized for use in COAMPS. The parameterization shows a plot of the collision efficiency for a single crystal with a radius of 800 μm. The red bold line shows a extension of the Wang and Ji results for droplets greater then the critical droplet radius (as determined by the point in the droplet spectrum where the droplet fall speed equals that of the ice crystal).

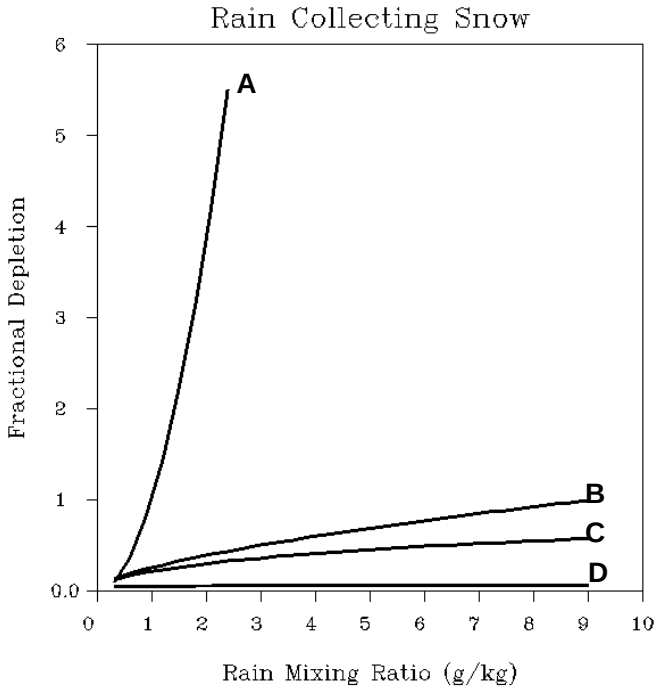

Figure 7. A plot of the fractional depletion of snow during a time step for the given rain water mixing ratio values and a model time step of 6 s. The snow mixing ratio was set to a fixed value of 1 g/kg. The symbols A,B,C,D refer to the various sensitivity runs as described in the text.

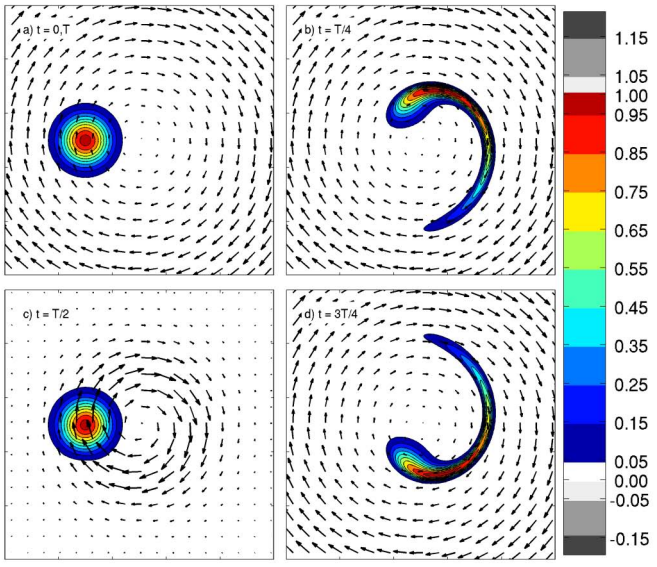

Figure 8. Illustration of the basic behavior of the exact solution.

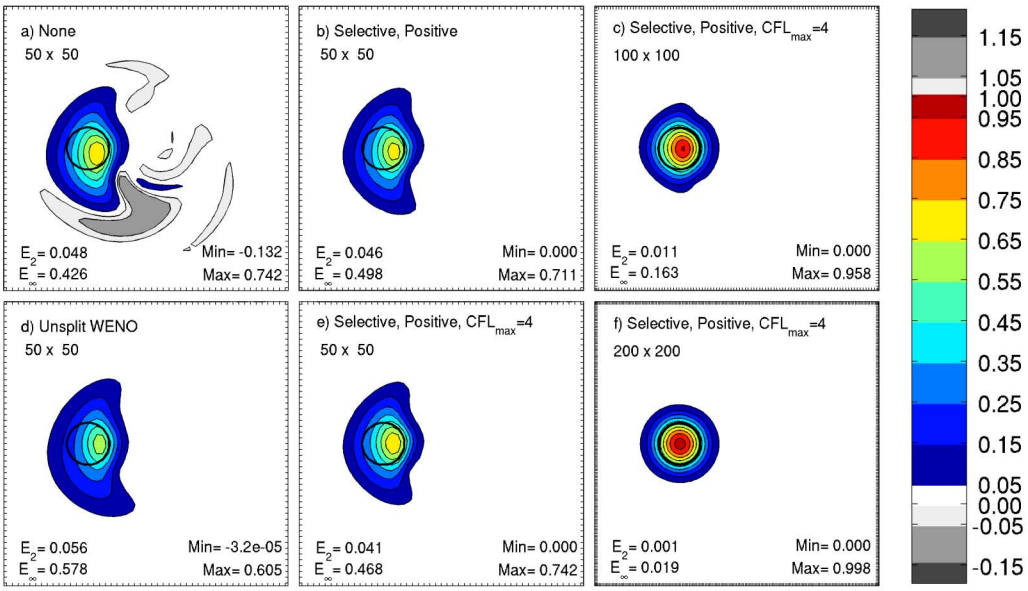

Figure 9. Numerical results generated by: (a) the unlimited PCM method, (b) the selectively limited PCM method with positivity preservation, (d) the standard WENO method, and (e) the selectively limited PCM method using a semi-Lagrangian framework with a maximum CFL number of 4. The total error in the mean-square sense (E_2) and the maximum norm (E_∞) is plotted in the lower left of each panel, the maximum and minimum values of the numerical solution (which can be compared with the correct values of 0 and 1) are plotted in the lower right. Finer resolutions of 100x100 (Fig. 9c) or 200x200 (Fig. 9f) are shown as well.